



ATLAS
EXPERIMENT



Cluster of Excellence
PRISMA⁺



FSP ATLAS
Erforschung von
Universum und Materie



Bundesministerium
für Bildung
und Forschung

JG|U

Measurement of Higgs boson differential and fiducial cross sections with the ATLAS detector

30.03.2023,

XXX International Workshop on Deep-
Inelastic Scattering and Related Subjects

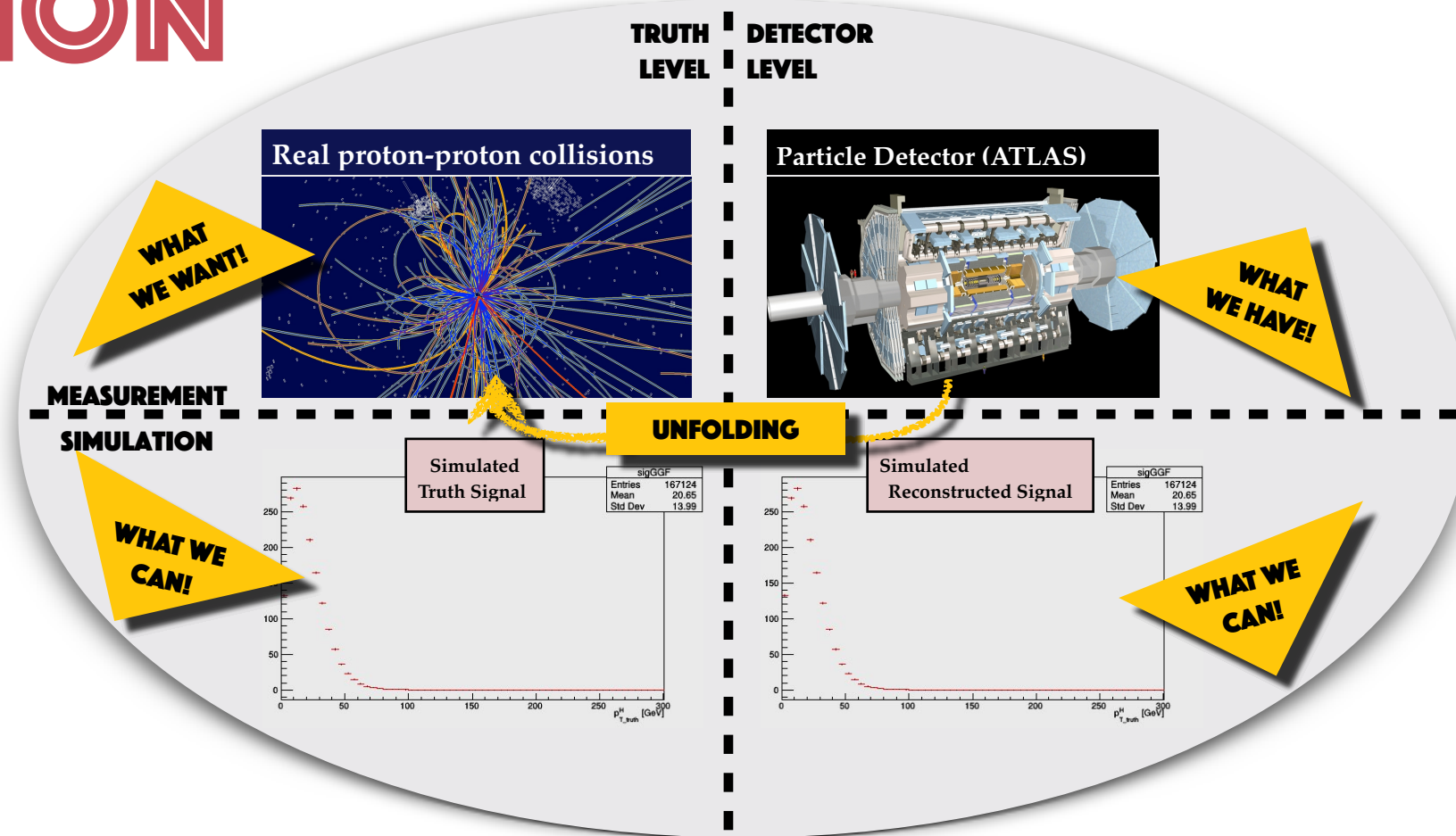
Anamika Aggarwal

INTRODUCTION

The Higgs Boson has been discovered in 2012 by both ATLAS and CMS experiments at the LHC, CERN.

● What after that?

- ✦ **precise measurements** of the properties of the Higgs Boson.
- ✦ investigate new methods to probe SM predictions and to test for the presence of **new physics**.



Differential and fiducial cross sections of Higgs Bosons in different production and decay channels:

- ➔ Deviations of Higgs properties from SM.
- ➔ Enhance sensitivity to BSM (Beyond SM) effects.
- ➔ Effects of higher-order corrections in perturbative theory.
- ➔ Provide constraints on different couplings.
- ➔ Different Higgs properties probed via different variables.

$$H \rightarrow \gamma\gamma$$

- Inclusive fiducial cross section: $\sigma_{\text{fid}} = 67 \pm 5 \text{ (stat.)} \pm 4 \text{ (sys.) fb}$ $\sigma_{\text{fid,SM}} = 64 \pm 4 \text{ fb}$
- Differential fiducial cross sections:
 - 20 differential cross-sections and 4 double-differential cross-sections in **inclusive diphoton fiducial region**.
 - 4 differential cross-sections and 1 double-differential cross-section in **VBF-enhanced region**.
 - Different variables sensitive to:
 - Higgs boson production kinematics,
 - jet kinematics,
 - spin, and CP quantum numbers of the Higgs Boson,
 - VBF kinematics and CP properties.
 - **New measurement** of the cross-section in the high $p_{\text{T}}^{\gamma\gamma}$ region:
 - Strongest limits to date for the Higgs boson production cross-section above 450 GeV.
 - All differential cross-sections compared with various SM predictions: No significant deviations found.

Variable

$$p_{\text{T}}^{\gamma\gamma}$$

$$|y_{\gamma\gamma}|$$

$$p_{\text{T}}^{\gamma^1}/m_{\gamma\gamma}$$

$$p_{\text{T}}^{\gamma^2}/m_{\gamma\gamma}$$

$$N_{\text{jets}}$$

$$N_{b\text{-jets}}$$

$$p_{\text{T}}^{j_1}$$

$$H_{\text{T}}$$

$$p_{\text{T}}^{\gamma\gamma j}$$

$$m_{\gamma\gamma j}$$

$$\tau_{C,j1}$$

$$\sum \tau_{C,j}$$

$$p_{\text{T}}^{\gamma\gamma, \text{jet veto } 30 \text{ GeV}}$$

$$p_{\text{T}}^{\gamma\gamma, \text{jet veto } 40 \text{ GeV}}$$

$$p_{\text{T}}^{\gamma\gamma, \text{jet veto } 50 \text{ GeV}}$$

$$p_{\text{T}}^{\gamma\gamma, \text{jet veto } 60 \text{ GeV}}$$

$$m_{jj}$$

$$\Delta\phi_{jj}$$

$$\pi - |\Delta\phi_{\gamma\gamma, jj}|$$

$$p_{\text{T}, \gamma\gamma jj}$$

$$\text{VBF-enhanced: } p_{\text{T}}^{j_1}$$

$$\text{VBF-enhanced: } \Delta\phi_{jj}$$

$$\text{VBF-enhanced: } |\eta^*|$$

$$\text{VBF-enhanced: } p_{\text{T}, \gamma\gamma jj}$$

$$p_{\text{T}}^{\gamma\gamma} \text{ vs } |y_{\gamma\gamma}|$$

$$(p_{\text{T}}^{\gamma^1} + p_{\text{T}}^{\gamma^2})/m_{\gamma\gamma} \text{ vs } (p_{\text{T}}^{\gamma^1} - p_{\text{T}}^{\gamma^2})/m_{\gamma\gamma}$$

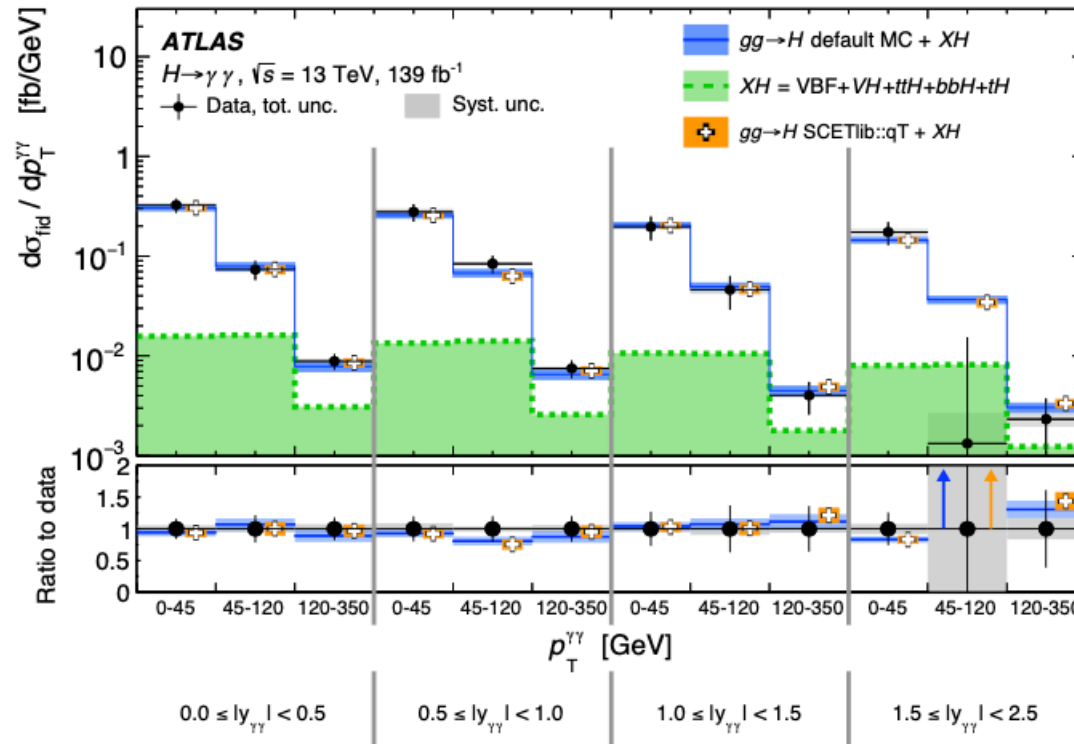
$$p_{\text{T}}^{\gamma\gamma} \text{ vs } p_{\text{T}}^{\gamma\gamma j}$$

$$p_{\text{T}}^{\gamma\gamma} \text{ vs } \tau_{C,j1}$$

$$\text{VBF-enhanced: } p_{\text{T}}^{j_1} \text{ vs } \Delta\phi_{jj}$$

arxiv:2202.00487

$$H \rightarrow \gamma\gamma$$



Interpretations:

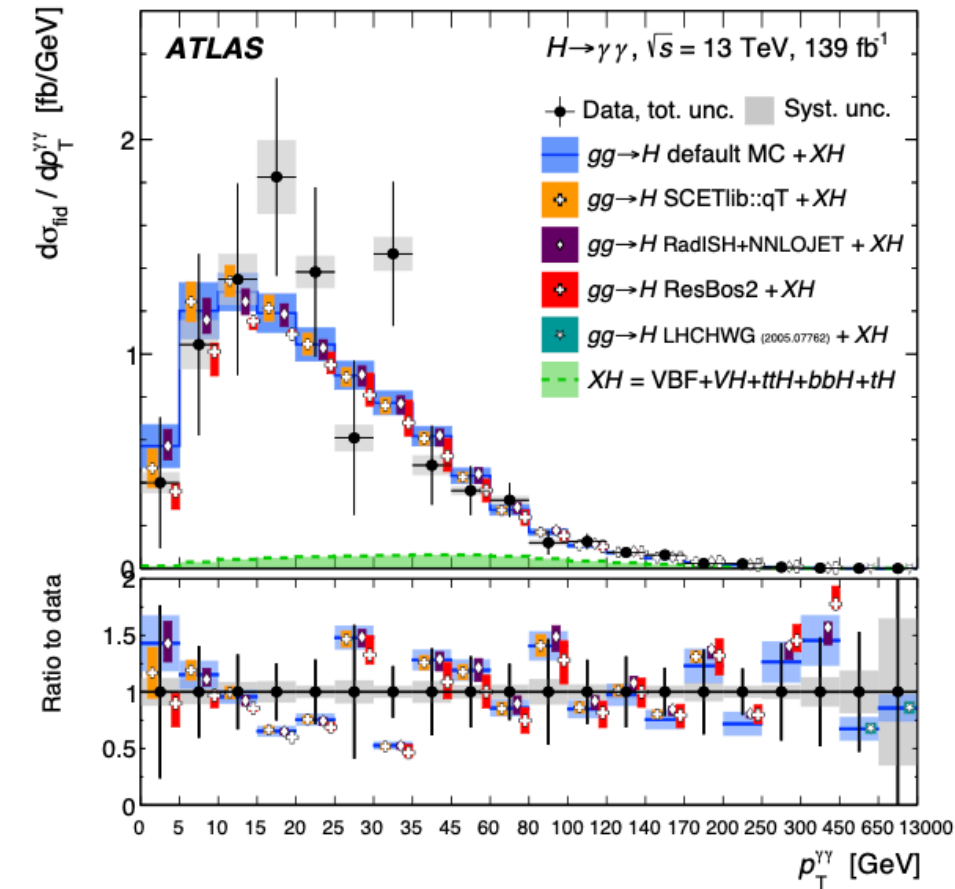
1. Measured transverse momentum distribution of the Higgs boson is used as an **indirect probe of the Yukawa coupling** of the Higgs boson to the bottom and charm quarks.

- 95% CL allowed range $[-3.7, 10.4]$ for κ_b , and $[-13.0, 18.9]$ for κ_c , using only the shape of transverse momentum distribution.

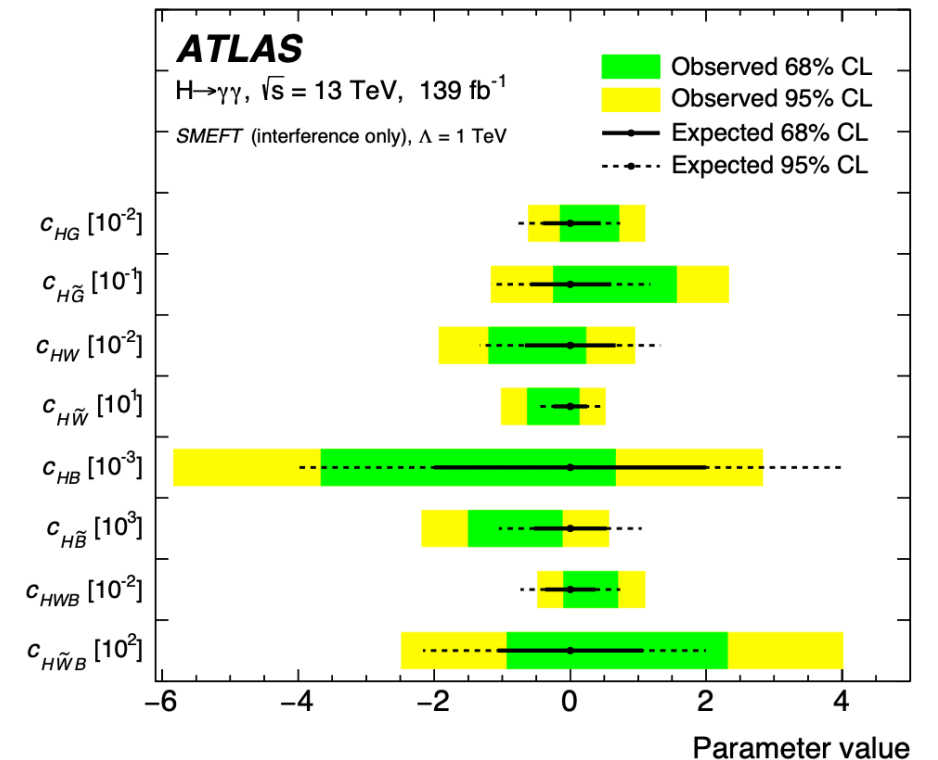
2. **Strength and tensor structure of the Higgs boson interactions** investigated using 5 variables in the effective field theory framework:

$$p_T^{\gamma\gamma}, N_{\text{jets}}, m_{jj}, \Delta\phi_{jj} \text{ and } p_T^{j_1}$$

- Constrain anomalous Higgs boson couplings to vector bosons in the Standard Model effective field theory framework.



Limits on SMEFT Wilson coefficients using SM and dimension-6 operators interference-only terms

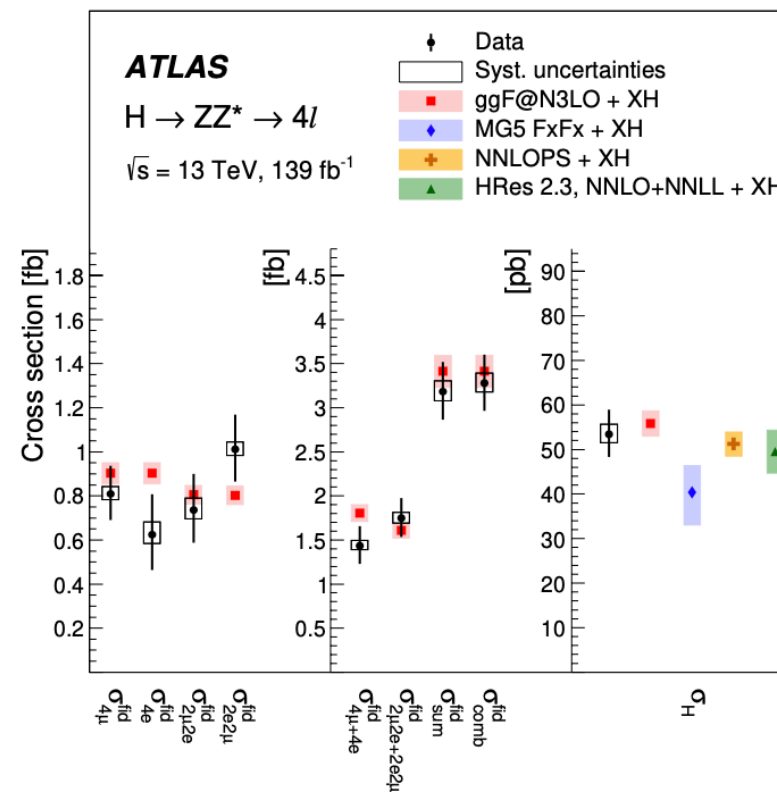


More Interpretations in combination with $H \rightarrow ZZ^* \rightarrow 4l$ on slide 8!

$$H \rightarrow ZZ^* \rightarrow 4l$$

| VBF-enriched region | Signal for cross-section estimates | Purity of VBF signal | Expected cross-section [fb] | Observed cross-section [fb] |
|---|------------------------------------|----------------------|--|--|
| $N_{\text{jets}} \geq 2, m_{jj} \geq 400 \text{ GeV}$ | All production modes | 59 % | $0.134^{+0.065}_{-0.053} {}^{+0.014}_{-0.012}$ | $0.215^{+0.075}_{-0.063} {}^{+0.016}_{-0.013}$ |
| $ \Delta\eta_{jj} \geq 3.0$ | VBF + VH + ttH | 95 % | $0.088^{+0.063}_{-0.053} {}^{+0.017}_{-0.020}$ | $0.172^{+0.072}_{-0.062} {}^{+0.016}_{-0.018}$ |

- Same-flavour opposite-charge (SFOC) lepton pairs selected to form Higgs boson candidates.
- All major background processes estimated from data.
- Inclusive fiducial cross section: $\sigma_{\text{fid}} = 3.28 \pm 0.30 \text{ (stat.)} \pm 0.11 \text{ (syst.) fb}$
 $\sigma_{\text{fid,SM}} = 3.41 \pm 0.18 \text{ fb}$
- Differential fiducial cross sections measured for a variety of observables sensitive to the production and decay of the Higgs boson.
- Signal events are corrected for detector measurement inefficiency and resolution by unfolding using the detector response matrix in the likelihood fit.
- Unfolding matrix used is well conditioned and no regularisation is required.
- An inclusive cross section in a VBF fiducial phase space is also measured.
- All measurements in agreement with the SM predictions.

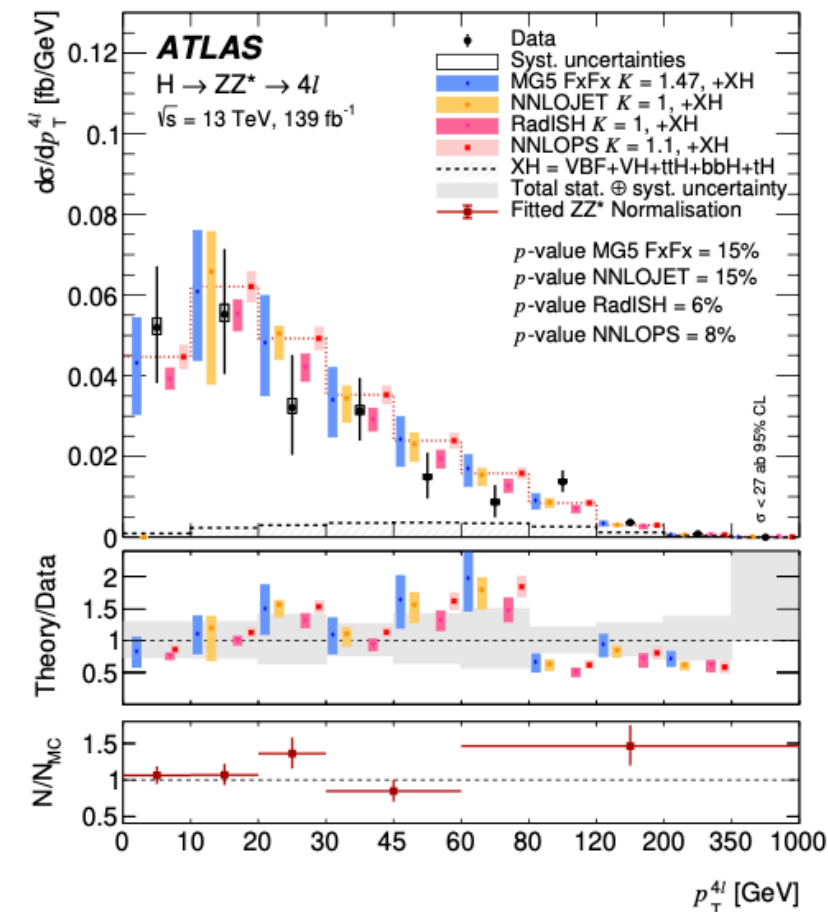
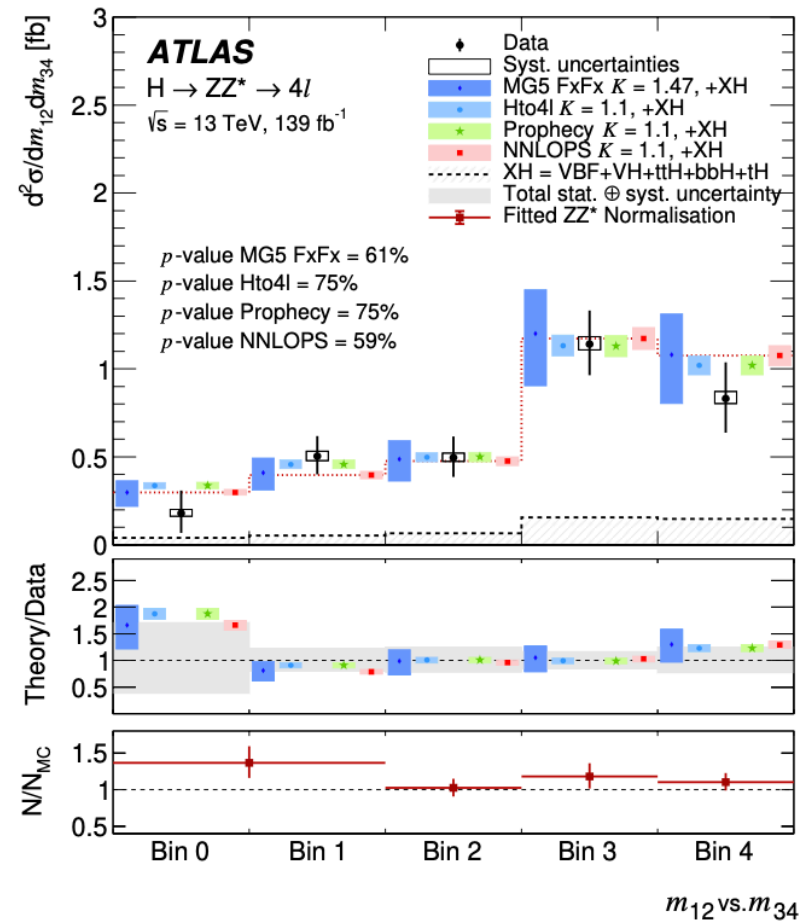


$$\begin{aligned}
 & p_T^{4\ell}, |y_{4\ell}| \\
 & m_{12}, m_{34} \\
 & |\cos \theta^*| \\
 & \cos \theta_1, \cos \theta_2 \\
 & \phi, \phi_1 \\
 & p_T^{4\ell j}, m_{4\ell j} \\
 & p_T^{4\ell jj}, m_{4\ell jj} \\
 & N_{\text{jets}}, N_{b\text{-jets}} \\
 & p_T^{\text{lead. jet}}, p_T^{\text{sublead. jet}} \\
 & m_{jj}, |\Delta\eta_{jj}|, \Delta\phi_{jj} \\
 & m_{12} \text{ vs. } m_{34}, p_T^{4\ell} \text{ vs. } |y_{4\ell}| \\
 & p_T^{4\ell} \text{ vs. } N_{\text{jets}}, p_T^{4\ell} \text{ vs. } p_T^{4\ell j} \\
 & p_T^{\text{lead. jet}} \text{ vs. } p_T^{\text{sublead. jet}} \\
 & p_T^{4\ell j} \text{ vs. } m_{4\ell j} \\
 & p_T^{\text{lead. jet}} \text{ vs. } |y^{\text{lead. jet}}|
 \end{aligned}$$

arxiv:2004.03969

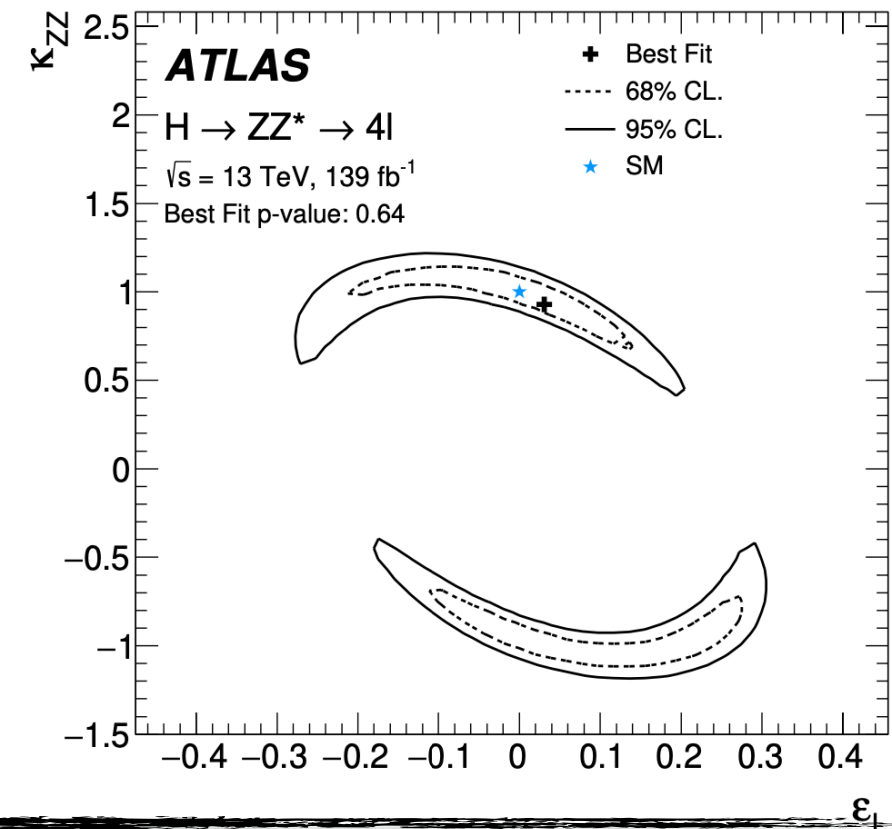
$$H \rightarrow ZZ^* \rightarrow 4l$$

Results used to constrain anomalous Higgs boson interactions with SM particles:



Observed limits on the modified Higgs boson decays within the linear EFT-inspired framework of the pseudo-observables

1. $m_{12} \text{ vs. } m_{34}$ double differential cross section used to **probe several BSM scenarios** within the framework of pseudo-observables
 - new and more stringent constraints on BSM scenarios where contact term interactions in the $H \rightarrow 4l$ amplitudes are set.
2. p_T^{4l} differential cross section used to **constrain the Yukawa couplings** of the Higgs boson with the b - and c -quarks
 - values of κ_c outside the range $\kappa_c \in [-12, +11]$ are excluded at 95% CL.

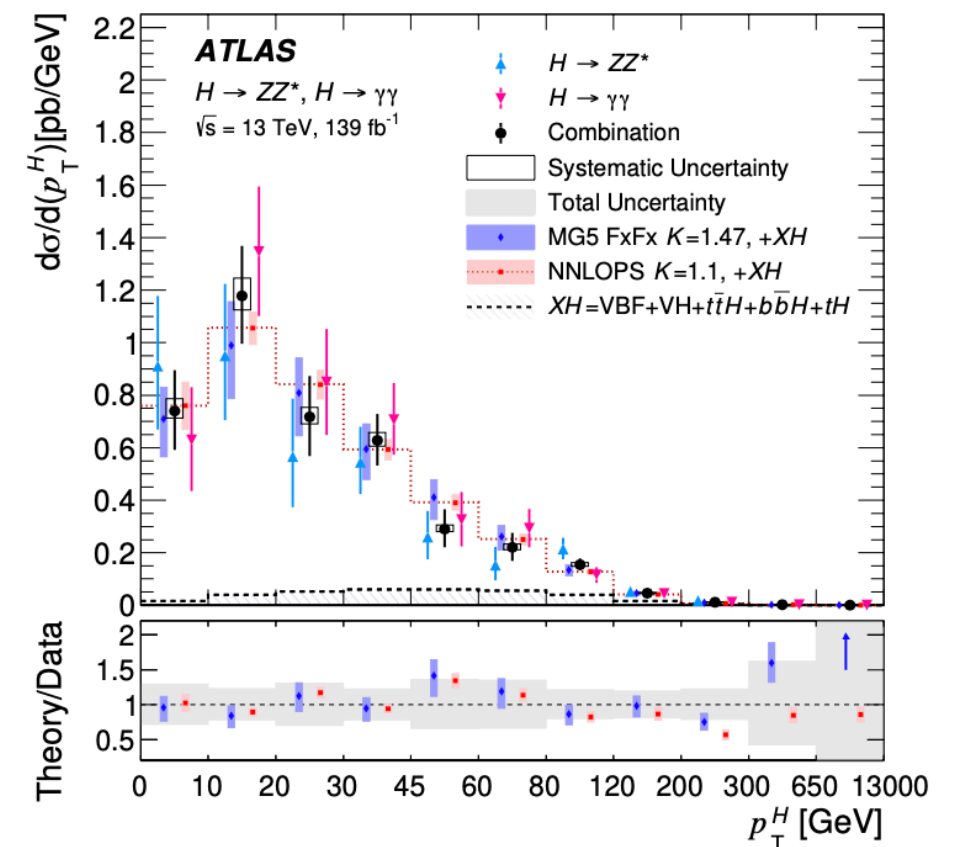


Combined $H \rightarrow ZZ^* \rightarrow 4l$ and $H \rightarrow \gamma\gamma$

- Measurements are **extrapolated to the full phase space** and the measured cross-sections are compared with SM predictions.
- Additional systematic uncertainties introduced by the extrapolation to the full phase space are counterbalanced by a **significant reduction of the statistical uncertainty** of the measurement (main limitation to the precision of the measurements in the individual decay channels).
- Total Higgs boson production cross-section: $55.5^{+4.0}_{-3.8}$ pb (± 3.2 (stat.) $^{+2.4}_{-2.2}$ (syst.)) $\sigma_{\text{fid,SM}} = 55.6 \pm 2.8$ pb

- Differential cross-sections:
 - $|y_H|$ sensitive to perturbative QCD calculations
 - p_T^H sensitive to the parton distribution functions (PDF)
 - N_{jets} and $p_T^{\text{lead. jet}}$ probe the theoretical modelling of high- p_T QCD radiation in Higgs boson production

All results from the two decay channels are compatible with each other, and their combination agrees with the Standard Model predictions.



[arxiv:2207.08615](https://arxiv.org/abs/2207.08615)

Combined $H \rightarrow ZZ^* \rightarrow 4l$ and $H \rightarrow \gamma\gamma$

Constraints on the b - and c -quark Yukawa couplings

1. Constraints from the Higgs boson transverse momentum distributions

- A joint interpretation, in terms of the b - and c -quark Yukawa coupling strengths to the Higgs boson, of the fiducial differential cross-sections measured as a function of p_T^H

2. Combination with the constraints from $VH(bb^-)$ and $VH(cc^-)$ production

- constraints set on the charm quark coupling modifier without any assumption on the bottom quark coupling.
- Represent the most stringent constraints on κ_C to date in these scenarios.

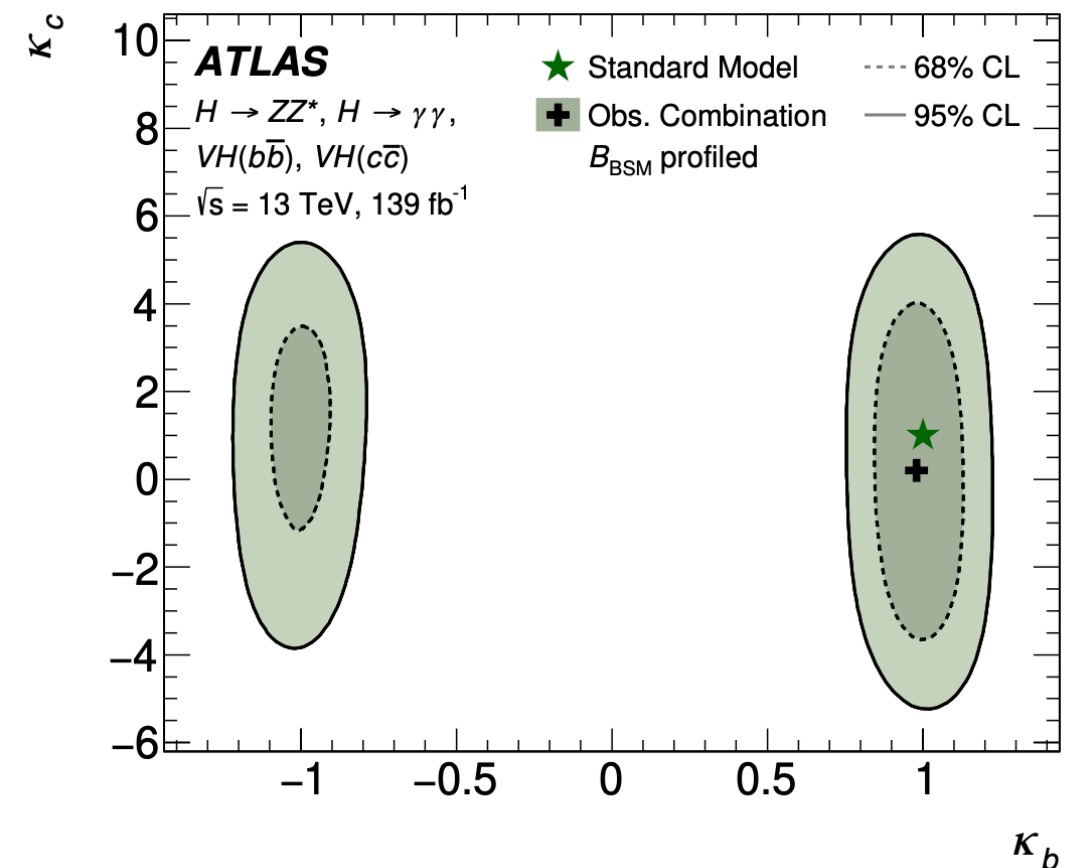
| Scenario | Observed 68% confidence interval | Observed 95% confidence interval |
|-----------------------------------|-------------------------------------|-------------------------------------|
| $B_{\text{BSM}} = 0$ | $[-1.61, 1.70]$ | $[-2.47, 2.53]$ |
| No assumption on B_{BSM} | $[-2.63, 3.01]$ | $[-4.46, 4.81]$ |

Assuming SM values of other couplings (κ)

| Parameter | Observed 95% confidence interval | Expected 95% confidence interval |
|------------|-------------------------------------|-------------------------------------|
| κ_b | $[-1.09, -0.86] \cup [0.81, 1.09]$ | $[-1.14, -0.92] \cup [0.86, 1.15]$ |
| κ_c | $[-2.27, 2.27]$ | $[-2.77, 2.75]$ |
| κ_b | $[-2.0, 7.4]$ | $[-2.0, 7.4]$ |
| κ_c | $[-8.6, 17.3]$ | $[-8.5, 15.9]$ |

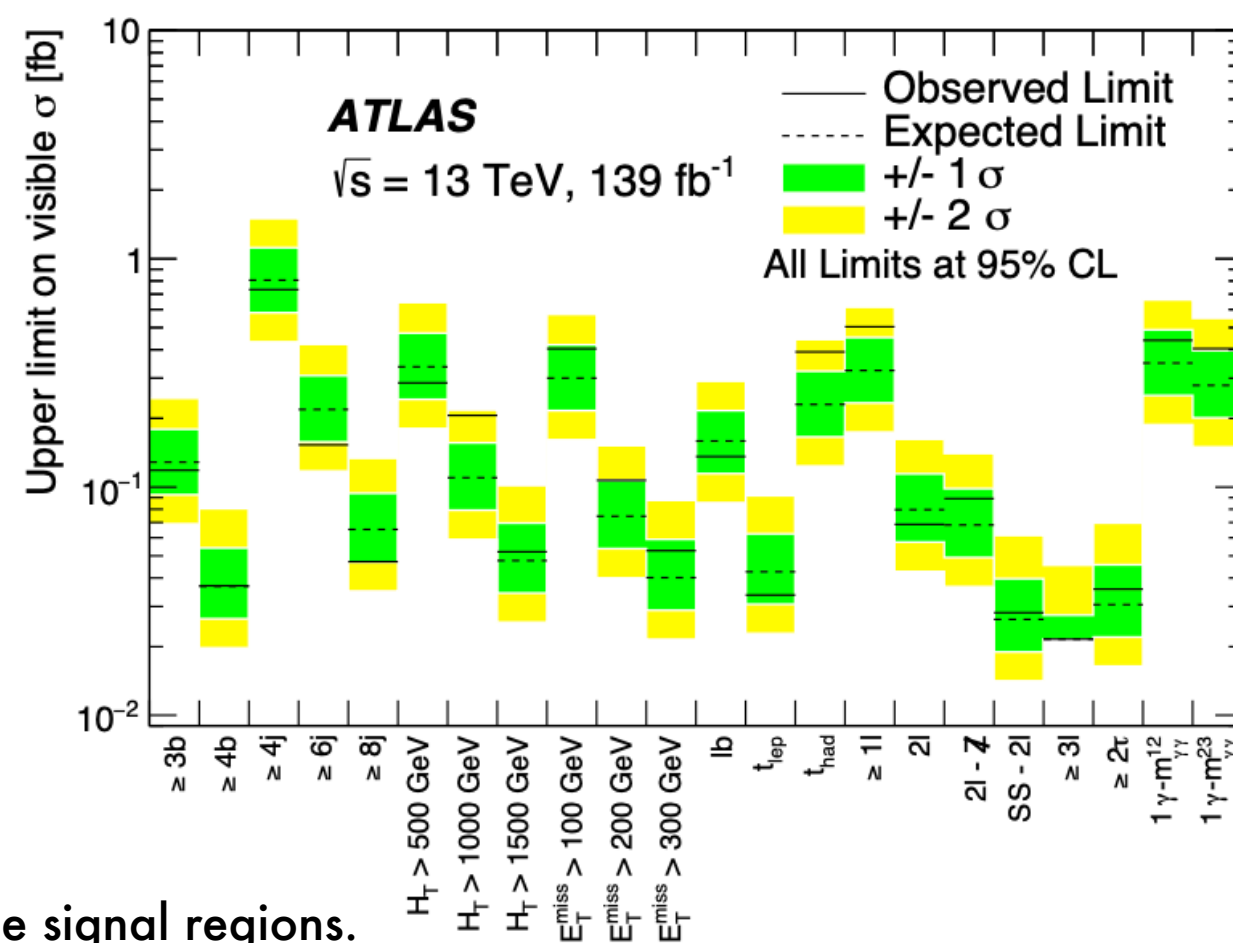
p_T^H shape and normalisation

p_T^H shape



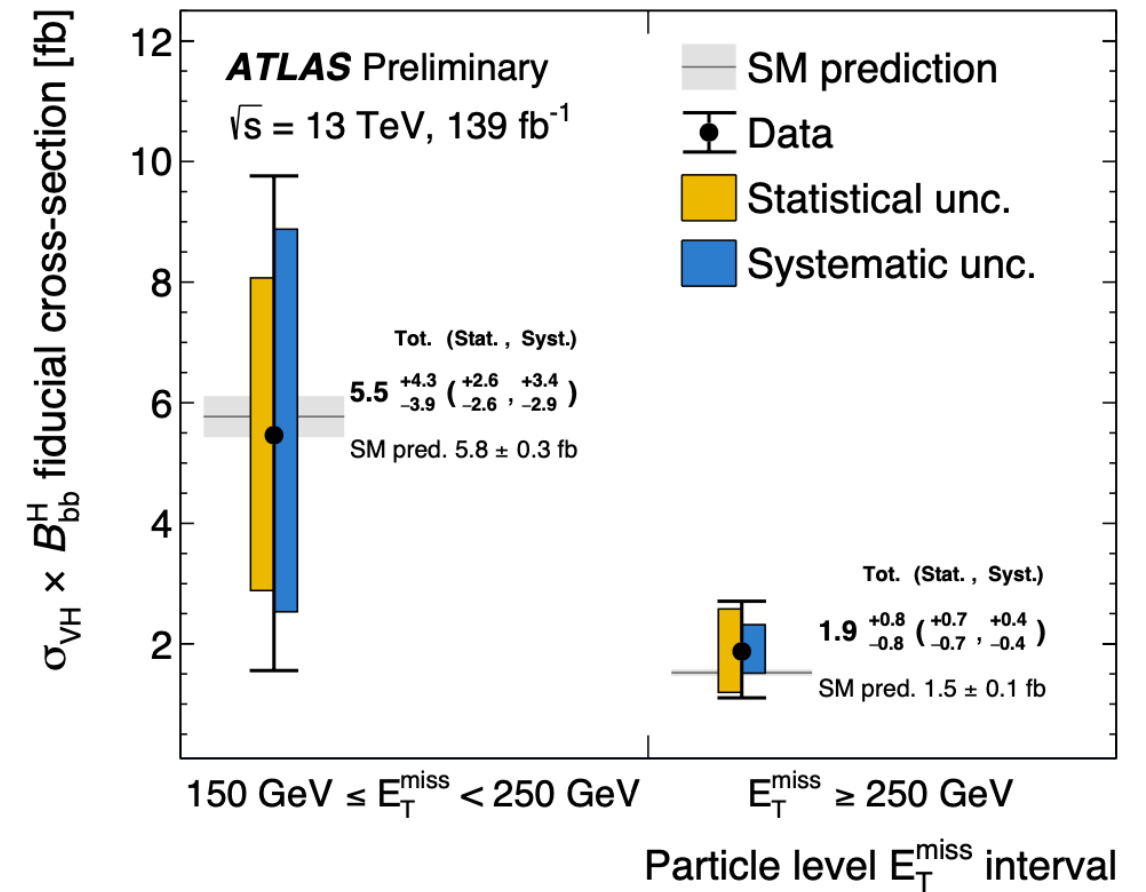
$$H \rightarrow \gamma\gamma + X$$

- Model-independent search for new physics leading to final states containing $H \rightarrow \gamma\gamma$ decays.
- Search examines **22 final states categorized by the objects** that are produced in association with the Higgs boson.
- Objects include
 - ▶ isolated **electrons** or **muons**,
 - ▶ hadronically decaying **τ -leptons**,
 - ▶ additional **photons**,
 - ▶ **missing transverse momentum**,
 - ▶ hadronic **jets**, as well as jets that are tagged as containing a b -hadron.
- No significant excesses above Standard Model expectations are observed.
- Upper limits at 95% CL were set on the visible cross section of BSM Higgs boson production in each of these signal regions.
- **Set of detector efficiency factors evaluated:**
 - ▶ Enables interpretation of the results as a constraint on other models.



$$H(bb) + E_T^{\text{miss}}$$

- First measurement of the fiducial cross-section of VH production ($V=W,Z$) in final states with missing transverse momentum where $H \rightarrow bb$.
- Cross-sections are reported for two intervals of missing transverse momentum, $150 \leq E_T^{\text{miss}} < 250 \text{ GeV}$ and $E_T^{\text{miss}} \geq 250 \text{ GeV}$.
- Results complement current cross-section measurements performed in the **STXS framework**, and provide a new way to probe $H \rightarrow bb$ decays.
- Measured fiducial cross section are in agreement with the SM expectations.



$150 \leq E_T^{\text{miss}} < 250 \text{ GeV}$ bin: $5.5 \pm 2.6 \text{ (stat.)} \pm 3.2 \text{ (syst.) fb}$
 $E_T^{\text{miss}} \geq 250 \text{ GeV}$ bin: $1.9 \pm 0.7 \text{ (stat.)} \pm 0.4 \text{ (syst.) fb}$

ggF

$$H \rightarrow WW^* \rightarrow e\nu\mu\nu$$

- Differential cross sections are measured in a fiducial phase space restricted to the production of **at most one additional jet**.
- Various observables in one and two-dimensions are measured which probe different properties of the Higgs Boson:
 - Higher-order QCD contributions to ggF production.
 - The spin structure and CP properties.
 - PDFs relevant for Higgs boson production.
 - Yukawa couplings of quarks and the Higgs boson.
- Signal region is defined using reconstructed objects and fiducial region is defined using particle-level objects.
- Fit is performed using the **profile likelihood method**.
- A signal region is defined for each bin of each observable, from which the number of signal events N_S is extracted from a fit to the data.
- A **combined fit is performed** in the m_T distribution in the range 80 to 160 GeV in bins of 10 GeV.

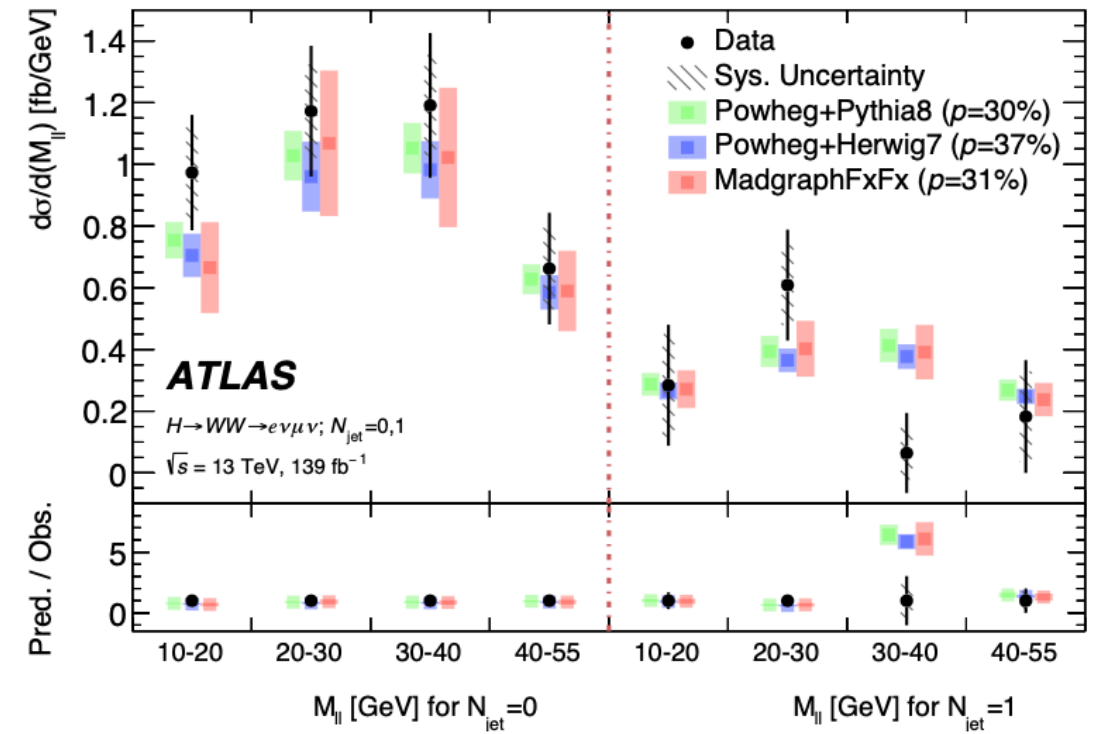
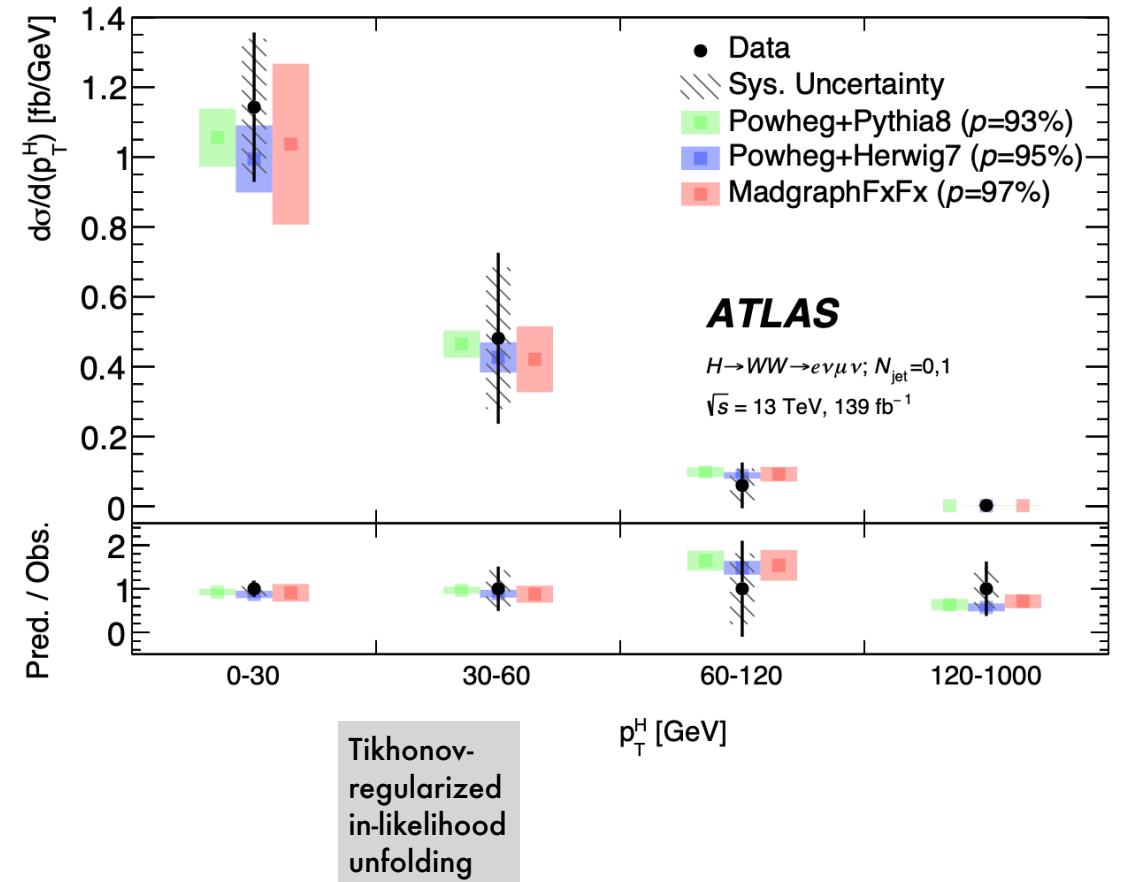
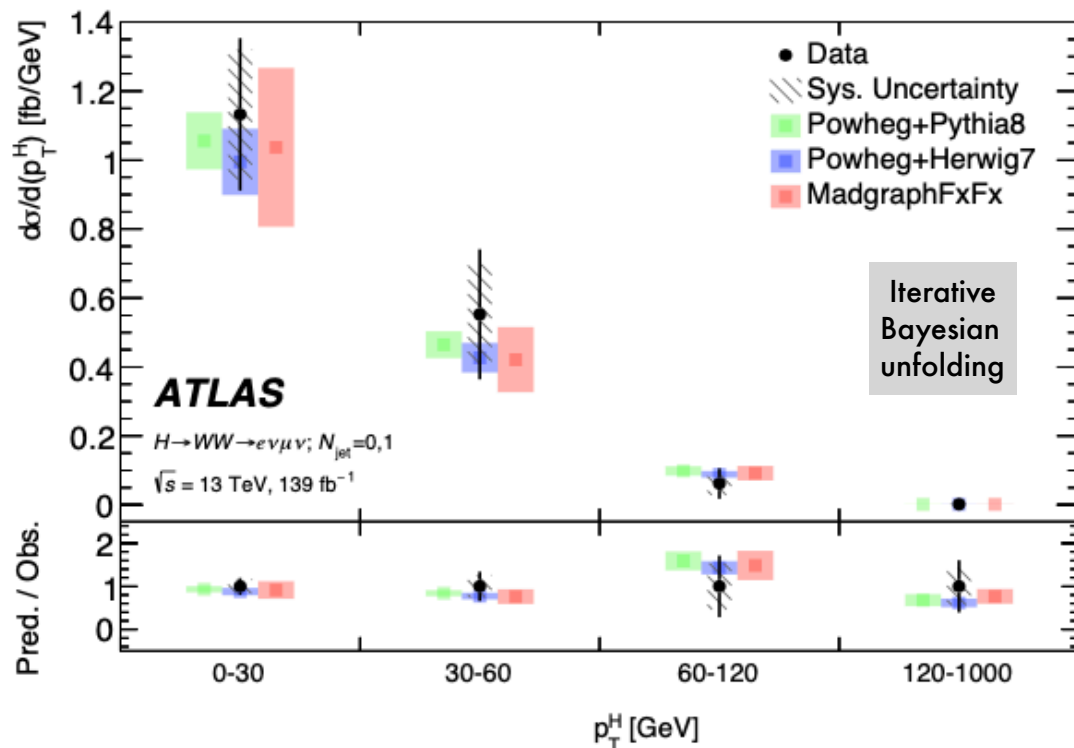
| |
|---|
| p_H^T |
| $M_{\ell\ell}$ |
| $p_{\ell\ell}^T$ |
| $y_{\ell\ell}$ |
| $\Delta\phi_{\ell\ell}$ |
| $\cos\theta^*$ |
| $p_{\ell 0}^T$ |
| y_{J0} |
| $M_{\ell\ell}$ versus N_{jet} |
| $p_{\ell\ell}^T$ versus N_{jet} |
| $y_{\ell\ell}$ versus N_{jet} |
| $\Delta\phi_{\ell\ell}$ versus N_{jet} |
| $\cos\theta^*$ versus N_{jet} |
| $p_{\ell 0}^T$ versus N_{jet} |

[arxiv:2301.06822](https://arxiv.org/abs/2301.06822)

ggF

$$H \rightarrow WW^* \rightarrow e\nu\mu\nu$$

- Tikhonov-regularized in-likelihood unfolding (and Iterative Bayesian unfolding as a cross check) is used to obtain the differential distributions.
- The results are consistent with Standard Model expectations, derived using different Monte Carlo generators.



VBF

$H \rightarrow WW^* \rightarrow e\nu\mu\nu$

**New
Results!**

- The cross sections are measured in a fiducial phase space.
 - Major processes extracted in data → minimisation of the background modelling uncertainties.
 - Multiple BDTs defined and trained to discriminate between signal and background processes, and BDT scores are used as templates in the fit to data.
 - Major backgrounds estimated in a simultaneous fit of the SR and CRs.
- Integrated fiducial cross section: $\sigma^{\text{fid}} = 1.68 \pm 0.40 \text{ fb} = 1.68 \pm 0.33 \text{ (stat)} \pm 0.23 \text{ (syst)} \text{ fb}$
- Differential measurements as a function of **13 variables** which probe different properties of the Higgs boson:
 - Higgs boson spin, charge, parity – QCD effects – EW corrections – BSM contributions
- Fit & matrix-inversion Unfolding to particle-level performed in a **single step of the Likelihood minimisation**.
- The uncertainties in the differential cross-section measurements are driven by the **data statistical uncertainty**.

$$\begin{array}{ccccccc}
 p_{\text{T}}^{\text{H}} & p_{\text{T}}^{\ell\ell} & p_{\text{T}}^{\ell_1} & p_{\text{T}}^{\ell_2} & m_{\ell\ell} & |\Delta y_{\ell\ell}| & |\Delta\phi_{\ell\ell}| \cos(\theta_{\eta}^*) \\
 p_{\text{T}}^{j_1} & p_{\text{T}}^{j_2} & m_{jj} & |\Delta y_{jj}| & \Delta\phi_{jj} & &
 \end{array}$$

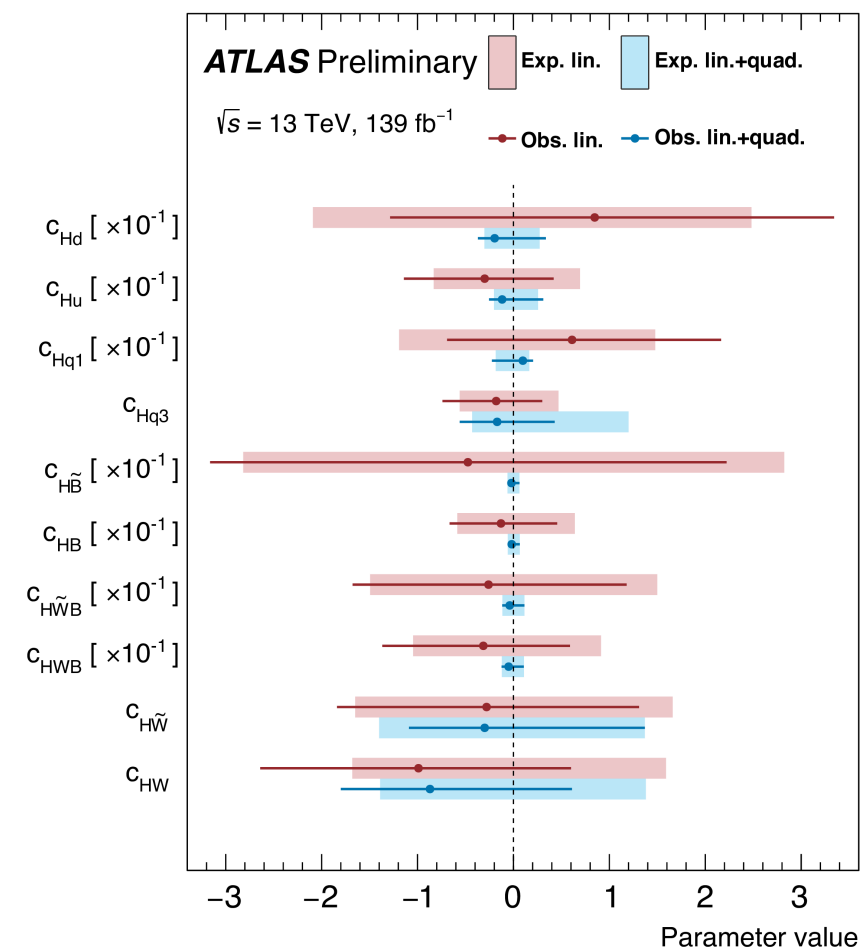
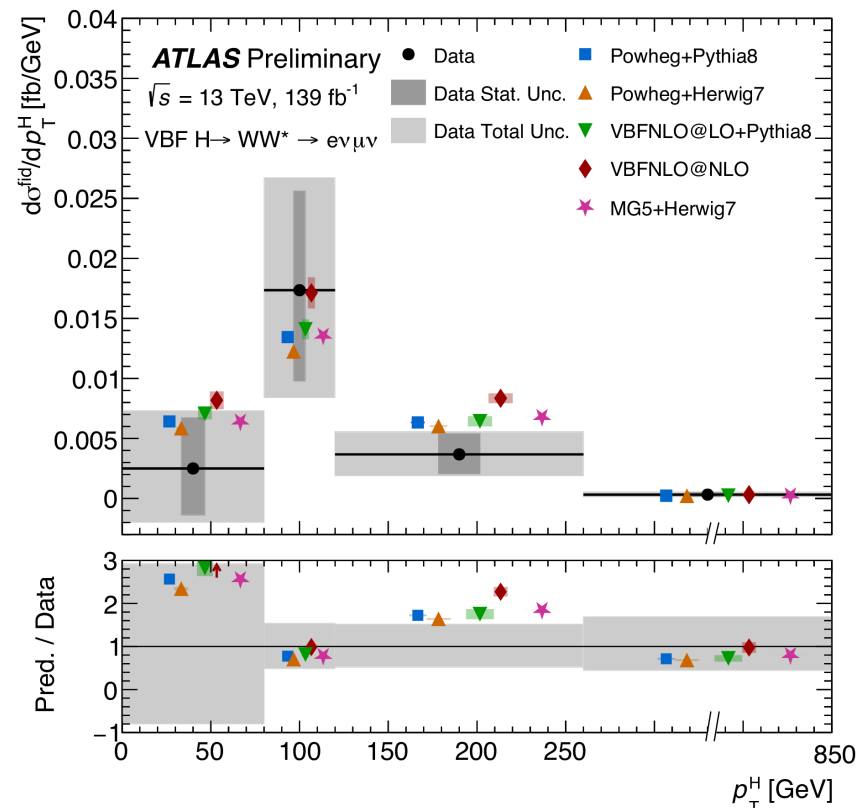
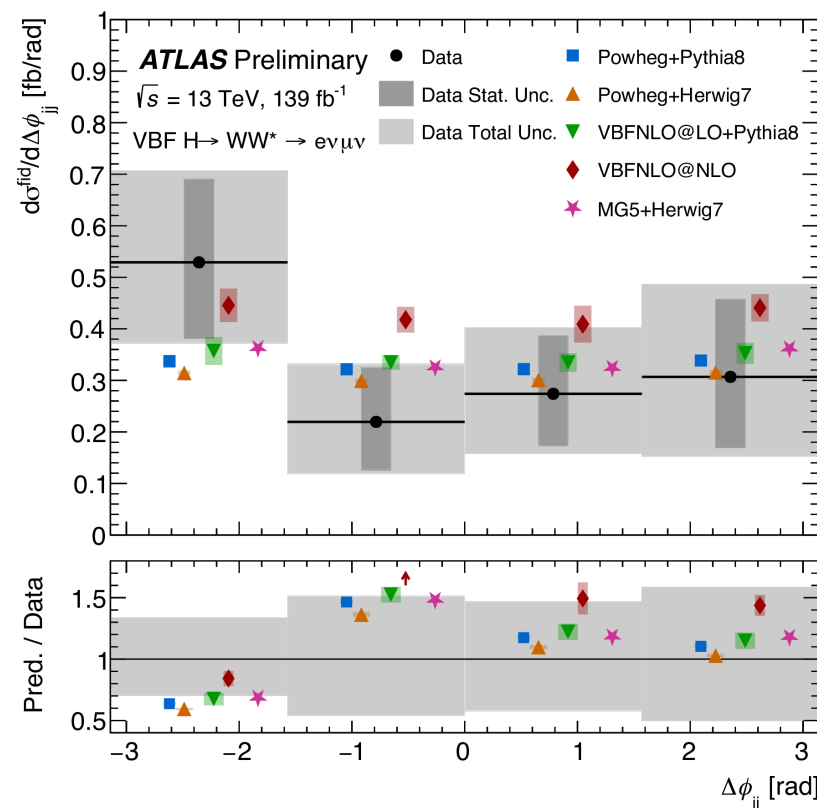
HIGG-2020-25

VBF

$$H \rightarrow WW^* \rightarrow e\nu\mu\nu$$

New Results!

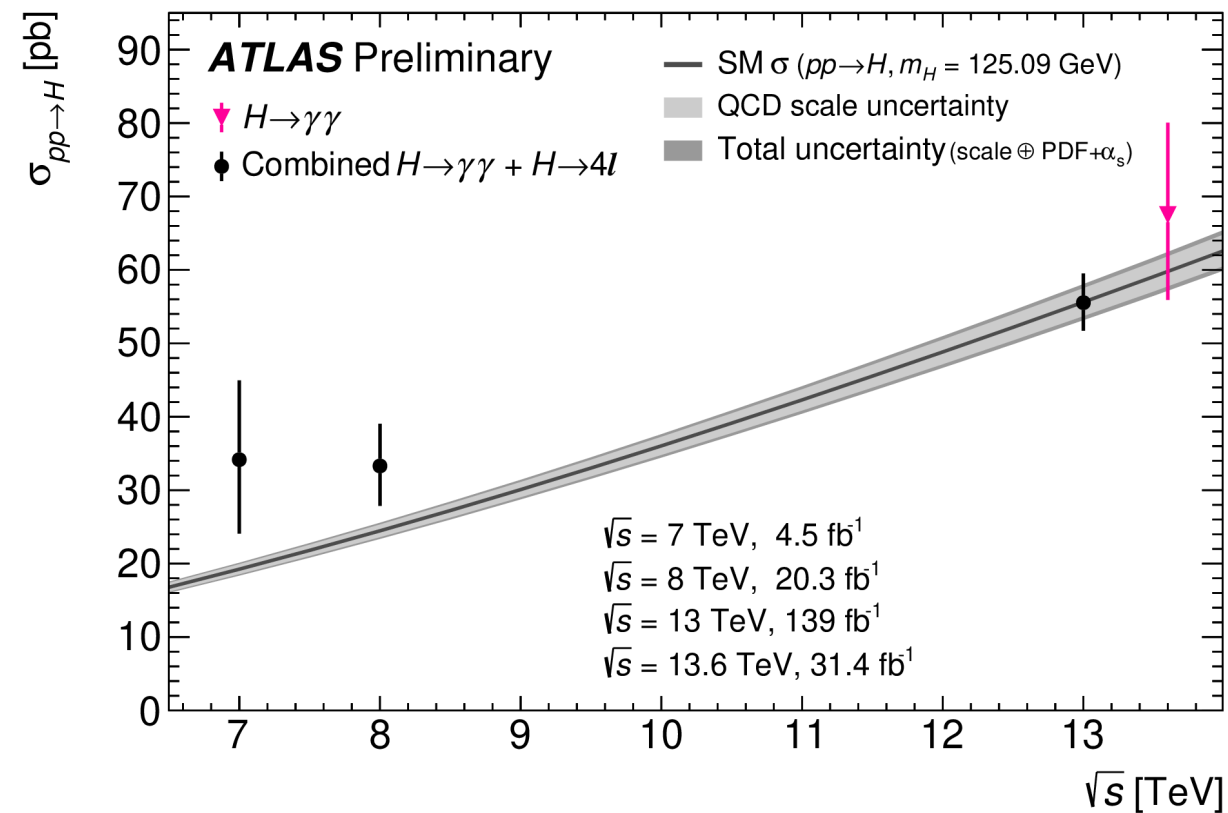
- Differential cross-sections are used to **constrain anomalous interactions** described by a dimension-six Effective Field Theory.
- Observed and expected values of SMEFT Wilson coefficients from CP-even and CP-odd operators.



$$H \rightarrow \gamma\gamma$$

$$\sqrt{s} = 13.6 \text{ TeV}$$

New Results!



- In 2022 the LHC has increased the centre-of-mass energy of the proton-proton (pp) collisions to the new **world-record value of 13.6 TeV**.
- About **31.4 fb^{-1}** of pp collision data recorded with the ATLAS detector.
- First ATLAS measurement of the $H \rightarrow \gamma\gamma$ cross-section at this new energy.**
- In order to reduce the model dependence, the measurement is restricted to a particle-level phase space matching closely the reconstruction-level photon kinematic selection, and it is corrected for detector effects:

$$\sigma_{\text{fid}}(pp \rightarrow H \rightarrow \gamma\gamma) = 76_{-13}^{+14} \text{ fb}$$

$$\text{SM } \sigma_{\text{fid}}(pp \rightarrow H \rightarrow \gamma\gamma) = 67.5 \pm 3.4 \text{ fb}$$

- Fiducial measurement is extrapolated to the full phase space:

$$\sigma(pp \rightarrow H) = 67_{-12}^{+13} \text{ pb}$$

$$\text{SM } \sigma(pp \rightarrow H) = 59.8 \pm 2.6 \text{ pb}$$

- These results do not show any significant deviation from the SM predictions.

ATLAS-CONF-2023-003

THANK YOU!